Available online at www.sciencedirect.com
ScienceDirect
C. R. Chimie 11 (2008) 332–339
COMPTES RENDUS CHIMIE
http://france.elsevier.com/direct/CRAS2C/

Account / Revue

Fungal prion proteins studied by solid-state NMR

Adam Lange, Beat Meier*

Physical Chemistry, ETH Zurich, CH-8093 Zurich, Switzerland

Received 29 May 2007; accepted after revision 9 August 2007
Available online 28 November 2007

Abstract

The progress of solid-state NMR obtaining atomic-resolution structural information for amyloid forming proteins is reviewed using the example of fungal prions. A detailed atomic resolution structure of an amyloid fibril is currently still missing. The main focus of this review is on the amyloid-forming fragment 218–289 of the prion protein HET-s of the filamentous fungus *Podospora anserina*. This prion exhibits the narrowest NMR resonance lines described so far for an amyloid and is therefore a favorable model system for such studies. Potential bottle-necks for three-dimensional structural determination, such as inherent conformational disorder, are discussed and the prospects for improvement in the methodological aspects and in sample preparation are discussed.
To cite this article: A. Lange, B. Meier, C. R. Chimie 11 (2008).

Keywords: Amyloid; Prion; HET-s; Solid state NMR; Magic angle spinning

1. Prions and amyloids

Prions are responsible for transmissible diseases where the agent is a conformationally altered protein of the host organism. Examples include chronic wasting disease in deer [1], scrapie in sheep [2], bovine spongiform encephalopathy (BSE) in cattle [3] or (new variant) Creutzfeldt–Jakob disease in man [4]. Prion diseases are believed to be associated with the formation of β-sheet rich aggregates, some of them forming amyloid fibrils.

Amyloid fibrils [5] are also associated with a number of different neurodegenerative diseases which are distinct from prion diseases and which are not believed to be transmittable. This class of diseases includes type 2 diabetes, Alzheimer's disease, Parkinson's disease, and Huntington's disease, to name a few [6]. It should, however, be pointed out that the classification into transmissible and non-transmittable disease is still a matter of debate [7,8].

Amyloid fibril formation can also be observed in *de novo* designed peptides [9] and appears to be a ubiquitous state of a polypeptide chain [10]. However, how this state is thermodynamically and kinetically related to the globular state and to the unfolded state of a protein is still unclear.

2. Structural aspects of prions in their amyloid state: the role of solid-state NMR

At the time of the writing of this document, no atomic resolution structure of an amyloid fibril has been published, although structural constraints have

* Corresponding author.
E-mail address: beat.meier@nmr.phys.chem.ethz.ch (B. Meier).

1631-0748/$ - see front matter © 2007 Académie des sciences. Published by Elsevier Masson SAS. All rights reserved.
doi:10.1016/j.crci.2007.08.014

been determined. Because of their size and shape, amyloid fibrils pose a challenge to the structural characterization by standard techniques for three-dimensional (3D) structure determination. X-ray diffraction patterns of partially aligned fibrils have resulted in the cross-β structure: a ribbon-like β-sheet that extends over the entire fibril with the individual β-strands aligned perpendicular to the fibril axis [11]. Small fragments of amyloid-forming peptides have been obtained in microcrystalline form and the crystal structure has been determined [12,13] but comparative solid-state NMR studies of the microcrystalline and fibrillar forms have shown that the structures are not identical [14].

The applicability of solution-state NMR spectroscopy is, due to the dimensions of the fibrils, limited. Nevertheless, important information has been gained by H/D exchange experiments: protonated fibrils are exposed to deuterated water for a given time interval and the H/D exchange is monitored after dissolution of the fibrils in aprotic solvents. The monomeric peptide is easily amenable to liquid-state NMR and the kinetics of H/D exchange reflects the formation of stable secondary structures in the fiber. The kinetics can be very slow with lifetimes in the order of months for well-formed β-sheets [15,16].

Recent progress in hardware (especially access to higher field strengths and faster MAS), methodology and sample preparation have enabled the spectral assignment and 3D structure determination of small globular proteins [17]. Examples include an SH3 domain [18], kaliotoxin [19,20], and ubiquitin [21,22]. Unlike solution-state NMR, solid-state NMR is not fundamentally restricted by a size limit. Thus, systems such as amyloid fibrils that form huge molecular weight complexes but are built up from small identical units can, in principle, be readily studied. Solid-state NMR has indeed already been applied to a variety of amyloid fibrils [16,23–28]. A recent review on amyloids is found in Ref. [5].

Nevertheless, limitations exist. Atomic-resolution NMR structure determination for solids is still not fully developed, even for crystalline proteins and, in the case of amyloids, is complicated by difficulties in distinguishing intra- from intermolecular interactions. In addition, amyloids in general and prions in particular tend to have slightly to significantly broader linewidths than good microcrystals [17]. For the fungal prion HET-s(218–289) a ^{13}C linewidth of 0.25–0.5 ppm was found [29] which rivals microcrystalline preparations. Other spectra from amyloids published so far are somewhat or significantly broader. Linewidths exceeding 1 ppm have been observed for example for Aβ [30], Ure2p(10–39) [31], and MoPrP(89–143) [32]. In the recent study of van der Wel et al. [14] comparably narrow ^{13}C linewidths in the order of 0.5–1.1 ppm have been reported for a segment of Sup35p. Whether this broader linewidth is a representation of a genuine structural disorder present in such systems (in silk, a related material [33,34], disorder is indeed an important feature [35]) or whether it is a consequence of non-optimal sample preparation remains to be investigated.

Solid-state NMR studies of infectious mammalian prions are complicated considerably by the fact that magic-angle sample rotation is required for high-resolution spectra with the inherent risk of rotor explosions and release of the agent into the environment. Therefore, fungal prions with no known toxicity and which, in part, appear naturally in our environment, are the most suited for initial investigations and the establishment of the method.

3. Fungal prions

Fungal prions include the three prions [URE3], [PSI], and [PIN] from the budding yeast *Saccharomyces cerevisiae* and the [HET-s] prion of *Podospora anserina*. The proteins expressed by these genes are Ure2p, Sup35p, Rnq1p, and HET-s, respectively. An excellent review covering a broad range of aspects of fungal prions has very recently appeared [36] and structural aspects have been reviewed in [37]. In the following we simply summarize some common aspects of these fungal prions before we discuss in some detail structural aspects of HET-s as seen from solid-state NMR.

In analogy to the mammal prion PrP [38–41], the above mentioned fungal prions consist of a globular and a prion-forming domain, the latter being disordered in the soluble form (corresponding to PrP^{C}) and suspected to be high in β-sheet content in the prion form (corresponding to PrP^{Sc}). If the fungal prion has a function (e.g. in Ure2p and Sup35p), the globular domain is the functional domain. The prion-forming domain is at one of the termini of the prion, the N-terminus for Ure2p, Sup35p, and the C-terminus for HET-s, Rnq1p, and PrP.

In the prion form, these proteins form filaments as do smaller fragments including the prion-forming domain. It is commonly assumed that all these fibrils can be described as being amyloids with a cross-β core, but this is subject of an ongoing discussion, in particular for Ure2p [36,42–44], where evidence for fibrils with and without amyloid character has been presented.

As mentioned in the introduction, no atomic-resolution structures of prions (and amyloids in general) in their fibrillar form are presently published. Nevertheless structural constraints are known from electron microscopy, circular dichroism, infrared spectroscopy and

NMR. Detailed information is given in Ref. [37]. Most studies propose an arrangement of multiple β-strands (with less than 20 residues each). An exemplary example is the β-arch model proposed by Tycko and coworkers [5], where each monomer consists of two β-strands linked by a short 180° turn that brings hydrophobic residues in both strands in close contact. Along the fibril axis the monomers stack in a parallel cross-β arrangement. A related model for the prion protein Ure2p, with 10 β-sheets per monomer (''parallel superpleated β-structure''), has been proposed by Kajava et al. [45]. As described in detail below, also the amyloid conformation of HET-s can be seen as stacking of two β-arches within one monomer. Amyloids containing β-arches can be looked at as a member of the class of β-solenoid proteins. Interestingly, for this class a wide variety of different cross-sections and a variable number of β-strands per layer (≥2) have been found [46].

4. HET-s

The system that we describe in detail in the following is the HET-s prion protein produced by the filamentous fungus *P. anserina*. This fungus can spontaneously undergo vegetative cell fusion events within the same but also between different individuals [47,48]. These cell fusion events lead to cytoplasmic mixing and to the formation of cells that contain different nuclear types (heterokaryons). Specific loci (e.g. het-s; see Table 1 for overview of HET-s notation) control the viability of these heterokaryons. Heterokaryotic cells formed between individuals of unlike het genotypes can be severely inhibited in their growth or even undergo a characteristic cell death reaction. The two different alleles *het-s* and *het-S* that are found at the locus het-s encode the proteins HET-s and HET-S. Strains of the *het-s* genotype exist in a non-prion phenotype [Het-s*] and a prion phenotype [Het-s]. On the other hand, there is only a non-prion phenotype [Het-S] of the *het-S* genotype. A heterokaryon formed by [Het-s*] and [Het-S] is viable, whereas heterokaryons of [Het-s] and [Het-S] are not. [Het-s*] strains can spontaneously convert to the [Het-s] phenotype. In addition, cell fusion between [Het-s] and [Het-s*] leads to a conversion of [Het-s*] to [Het-s]. These properties are due to the prion nature of HET-s, which can serve as a model protein for the study of amyloid assembly and prion propagation [2]. Even though the exact mechanism of the cell death reaction is not known, it has been hypothesized that the non-prion HET-S incorporates into the HET-s fibrils and inhibits further aggregation. In this theory the toxic species are the smaller aggregates of HET-s and HET-S and not the full-length HET-s fibrils [47,48]. A similar mechanism could in principle also be conceivable for amyloid diseases.

Table 1
HET-s notations

het-s	Gene locus
het-s/*het-S*	Different alleles
[Het-s*] and [Het-s]/[Het-S]	Phenotypes
HET-s/HET-S	Proteins

The HET-s prion protein is 289 amino acids long. It differs in only 13 residues from HET-S. Biolistic introduction of amyloid fibrils formed by HET-s into [Het-s*] strains can induce the [Het-s] phenotype [49,50]. Also the protease K resistant core of the fibrils that is formed by the C-terminal residues 218–289 is prion infective. In solution, HET-s(218–289) is unstructured [47]. The conformation of HET-s(218–289) in its fibrillar state has recently been studied by a combination of solid-state NMR spectroscopy [29], H/D exchange, and mutant and water accessibility studies [16]. The study resulted in a model of the HET-s(218–289) protein in its fibrillar state. In this model the structural unit of HET-s amyloids consists of four β-strands that are arranged in a β-solenoid arrangement (see Fig. 1).

The model is based on information from solid-state NMR chemical shifts of Cα and Cβ atoms (indicative of secondary structure; can be obtained unequivocally from well resolved two-dimensional spectra; see e.g. Fig. 2), H/D exchange experiments in combination with solution-state NMR (identification of solvent-protected backbone amide protons involved in hydrogen bonds) and fluorescence studies (indicating which residues are solvent-exposed). The model is in agreement with point mutant and deletion studies and recent mass-per length measurements [51]. The mass-per-length measurements indicate that the fibrils consist of a stack of single protein molecules continued along the fibril direction. This finding is in contrast to other

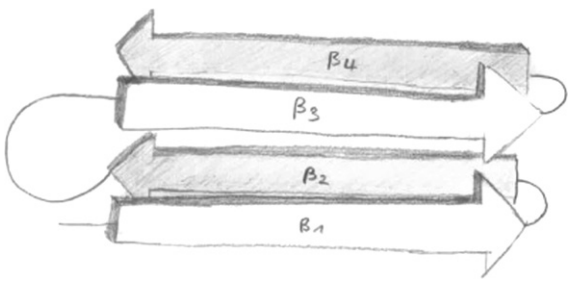

Fig. 1. Cartoon representation of the β-solenoid arrangement of the HET-s(218–289) protein in its fibrillar form. Artwork: courtesy of Ansgar Siemer.

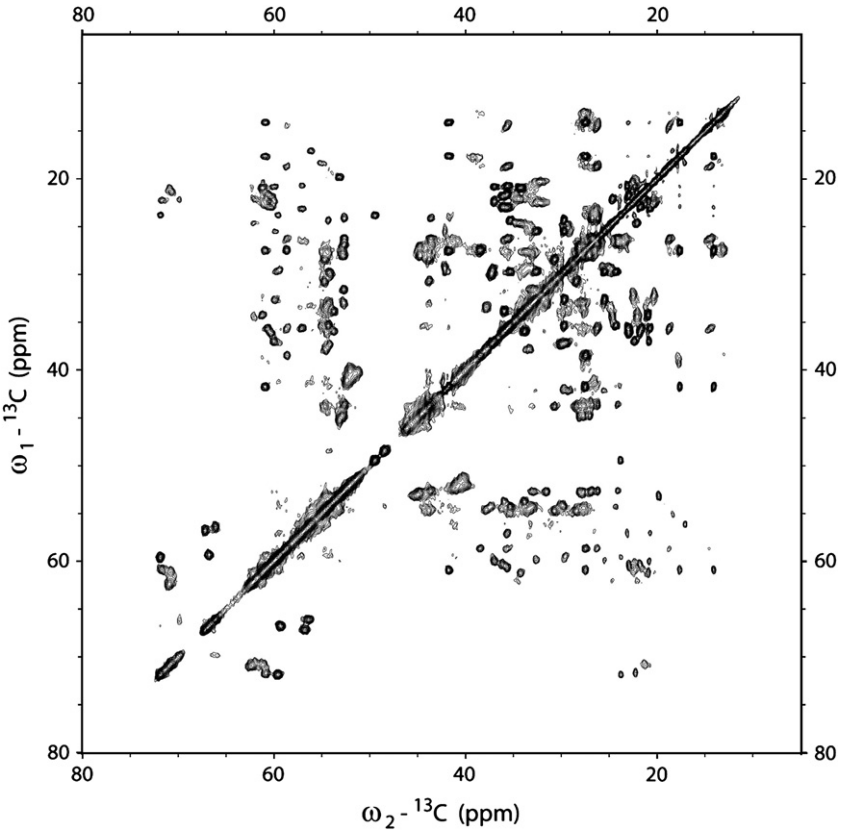

Fig. 2. $^{13}C-^{13}C$ correlation spectrum of HET-s(218–289) amyloid fibrils (PDSD with a mixing time of 100 ms). The spectrum was recorded on a 850 MHz wide-bore spectrometer (Bruker Biospin, Germany) at a probe temperature of −10 °C and at 19 kHz magic-angle spinning.

amyloids where the fibrils are ''thicker'' than a single molecule, often with the number of molecules stacked perpendicular to the fibril axis being variable (see Ref. [9] for an example) and possibly inducing an element of disorder. The model of Ritter et al. is supported by numerous through-space distance constraints between the backbone carbons of the β1 and β3 strands and between side chains of the β1 and β2 strands (unpublished data, presented at the XII ICMRBS, Göttingen). However, a detailed atomic structural model has not yet been presented. Interestingly, the N- and C-termini and the long loop between β2 and β3 (see Figs. 1 and 3) seem to be dynamically disordered [52]. The precise biological role of these flexible parts is not known.

Based on the data that are already known from Ritter et al. different possible supra-molecular arrangements can be imagined. An important experimental observation for these considerations is the fact that only one set of NMR frequencies is observed. This can only be true if all monomers in the fibril have (a) exactly the same conformation and (b) exactly the same inter-monomer interface. Two models that fulfill this requirement are shown in Fig. 3. Both parallel and anti-parallel supra-molecular arrangements are conceivable. The supra-molecular structure of the HET-s(218–289) fibrils could be determined experimentally by a combination of solid-state NMR spectroscopy and isotope labeling. For example, NHHC [53,54] experiments can be performed on samples that are a mixture of U-[^{13}C] labeled

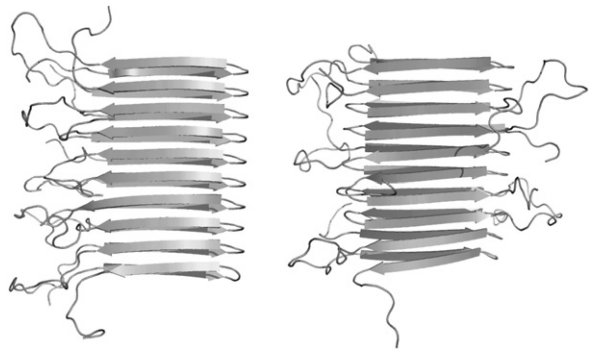

Fig. 3. Models of HET-s(218–289) fibrils assuming a symmetric (left panel) and antisymmetric (right panel) supra-molecular arrangement, respectively. Each monomer consists of rigid (four β-strands) and flexible (N-, and C-termini, loop) parts.

HET-s(218–289) and U-[^{15}N] labeled HET-s(218–289). In this type of sample the NHHC cross peaks that arise in the spectrum are a direct probe of the intermolecular interface between the individual monomers and thus, can be used to infer the supra-molecular arrangement [55]. In addition, a comparison of CHHC [53,54] spectra on diluted and CHHC spectra that are recorded on undiluted samples can be used to assign intermolecular cross peaks. These will only be observed in the spectra of the undiluted samples. Similarly, a comparison of ^{13}C proton-driven spin diffusion spectra of diluted and undiluted samples will yield additional information.

Solid-state NMR methods can also be utilized to study the flexible parts of the HET-s amyloids. Initial HRMAS experiments indicate that some 15 residues in a loop that connects two of the four β-strands and N- and C-terminal residues are flexible [52]. However, up to now no sequential assignment of these flexible residues has been obtained. The main reasons for this are (a) the spectral overlap of resonances that results from all flexible residues being in a random coil conformation and (b) the difficulty to obtain NOESY constraints. In addition, ^{13}C detected experiment as described by Andronesi et al. [56] can be performed. In contrast to usual solid-state NMR experiments that are based on an initial cross-polarization step these experiments utilize an INEPT transfer. In this case only mobile residues that have long enough transverse dephasing times T_2 will be visible. As an example a ^{1}H–^{13}C INEPT spectrum is shown in Fig. 4.

5. Potential for methodological improvements

Applications of solid-state NMR to prions, other amyloids as well as biological applications in general have only been made possible by improvements in resolution and sensitivity and sample-preparation techniques. Still, these issues are far from being fully solved and there is considerable potential for significant improvements in the years to come. The magnetic field strength available for NMR experiments will continue to increase with the associated improvements in resolution and sensitivity. Our lab has recently commissioned a 20 Tesla wide-bore magnet (at 850 MHz ^{1}H larmor frequency, Bruker Biospin, Karlsruhe, Germany) and the spectra of HET-s(218–289) amyloid fibrils show indeed a significantly improved spectral resolution when compared to 600 MHz data. Fig. 5b shows a ^{15}N–^{13}C correlation spectrum of HET-s(218–289) amyloid fibrils that was recorded at 850 MHz. In contrast to older data (Fig. 5a), basically all resonances of the rigid parts of HET-s are observed and can be assigned unambiguously. Due to the large dispersion of ^{13}C NMR frequencies in proteins the ^{13}C dimension usually exhibits the highest resolution that can be obtained in solid-state NMR. Consequently two-dimensional spectra with two ^{13}C dimensions can be very well resolved. As an example Fig. 2 shows a PDSD spectrum that was recorded at 850 MHz ^{1}H larmor frequency. The high resolution is a necessity if structural constraints from two-dimensional data sets are to be obtained. Here, two-dimensional cross peaks can be only assigned unambiguously if both resonance frequencies are specific.

The improvements in signal-to-noise ratio seem to be about what is expected $(850\ \text{MHz}/600\ \text{MHz})^{3/2} = 1.7$, but a detailed comparison is presently not available. While further increases in the static magnetic field will undoubtedly further increase the signal-to-noise ratio, the improvements in spectral resolution are harder

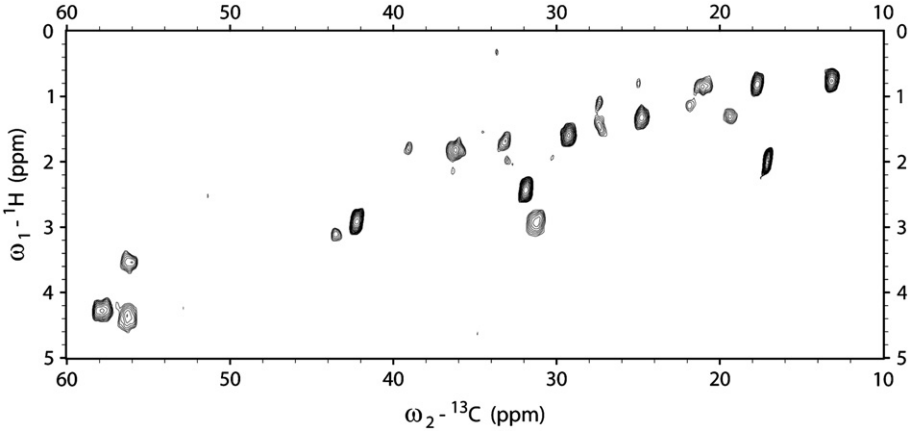

Fig. 4. ^{1}H–^{13}C INEPT spectrum of HET-s(218–289) amyloid fibrils. The spectrum was recorded on a 600 MHz wide-bore spectrometer (Bruker Biospin, Germany) at a probe temperature of 0 °C and at 10 kHz magic-angle spinning.

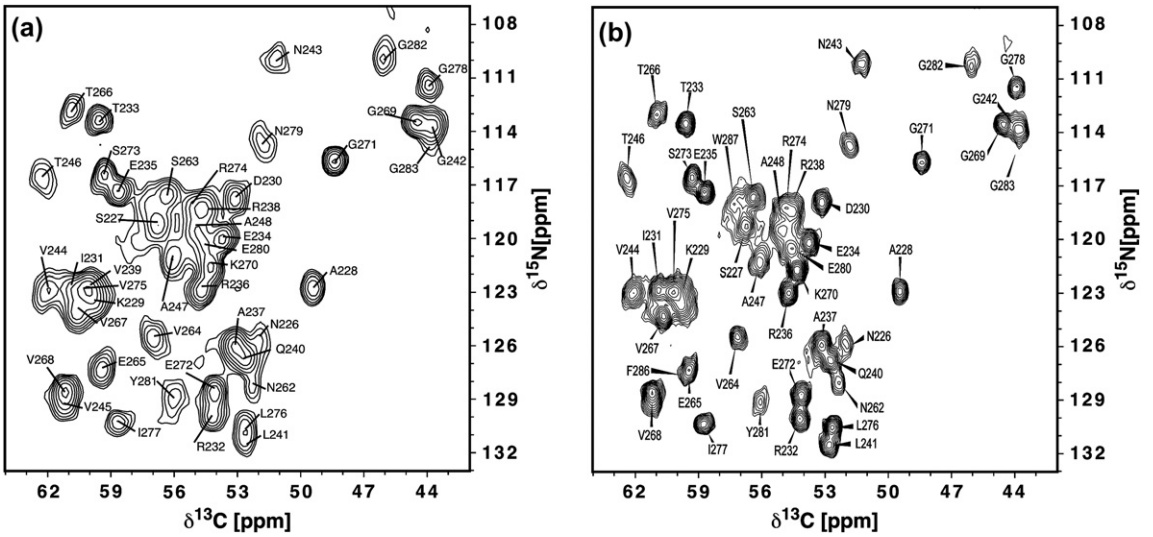

Fig. 5. (a) $^{15}N-^{13}C$ correlation spectrum of HET-s(218–289) amyloid fibrils. The spectrum was recorded on a 600 MHz wide-bore spectrometer (Bruker Biospin, Germany) at a probe temperature of +10 °C and at 40 kHz magic-angle spinning (spectrum reprinted from PhD thesis of Ansgar Siemer, DISS. ETH No. 16916); (b) $^{15}N-^{13}C$ correlation spectrum of HET-s(218–289) amyloid fibrils. The spectrum was recorded on a 850 MHz wide-bore spectrometer (Bruker Biospin, Germany) at a probe temperature of −10 °C and at 19 kHz magic-angle spinning.

to predict. They depend on the mechanism that dominates the line broadening. Some mechanisms, like non-resolved homonuclear couplings and some contributions from imperfect heteronuclear decoupling are field independent. Because the chemical-shift dispersion increases linearly with the static field strength, the resolution in spectra with a linewidth determined by such mechanisms improves linearly with the magnetic field strength. There are also other broadening mechanisms, including contributions to the remaining dipolar coupling and bulk susceptibility effects, which depend linearly on the magnetic field. Such spectra will show no improved resolution in higher fields. A particularly important mechanism of the latter type is the line broadening caused by disorder in the sample. Disorder leads to a distribution in isotropic chemical shifts and the resulting linewidth is, expressed in ppm of the field strength, independent of the field. The uniformity of the sample is, therefore, an ultimate limit for the resolution of solid-state NMR spectra. While highly resolved spectra will ultimately lead to atomic-resolution structures, poorly resolved spectra will only be interpretable with considerable investment into the production of selectively labeled compounds.

6. Conclusions and outlook

The high local order detected for HET-s(218–289) shows that at least this fragment of a fungal prion is clearly amenable to atomic structure determination by solid-state NMR. So far, published spectra of other prion proteins – all of them being relatively small fragments – show broader lines. The same was observed for a fragment of a mammal prion [57]. The linewidth observed still allow for structural characterization in these systems but high-resolution structure determination from a single or a few multidimensional NMR spectra is complicated in the case of severe spectral overlap. At this point in time it is not clear, if improved sample-preparation techniques will enhance the spectral resolution or if the present linewidth represents a native disorder inherent in these systems.

In cases where narrow line widths can be obtained we expect that solid-state NMR spectroscopy will prove to be successful in obtaining high-resolution structures of amyloid fibrils formed by prion proteins. High-resolution structural information would be very beneficial for the understanding of amyloid formation and prion propagation. Such results could also prove to be useful in the context of inhibitors of amyloid fibril growth and drug development related to amyloid diseases.

Acknowledgements

We thank Hélène van Melckebeke, Christian Wasmer, Ansgar Siemer, and Matthias Ernst for helpful discussions. Financial support by the ETH Zurich

through the TH-grant system and by the Swiss National Science Foundation is gratefully acknowledged.

References

[1] C.K. Mathiason, J.G. Powers, S.J. Dahmes, D.A. Osborn, K.V. Miller, R.J. Warren, G.L. Mason, S.A. Hays, J. Hayes-Klug, D.M. Seelig, M.A. Wild, L.L. Wolfe, T.R. Spraker, M.W. Miller, C.J. Sigurdson, G.C. Telling, E.A. Hoover, Science 314 (2006) 133.
[2] S.B. Prusiner, Science 216 (1982) 136.
[3] G.A.H. Wells, A.C. Scott, C.T. Johnson, R.F. Gunning, R.D. Hancock, M. Jeffrey, M. Dawson, R. Bradley, Vet. Rec. 121 (1987) 419.
[4] R.G. Will, J.W. Ironside, M. Zeidler, S.N. Cousens, K. Estibeiro, A. Alperovitch, S. Poser, M. Pocchiari, A. Hofman, P.G. Smith, Lancet 347 (1996) 921.
[5] R. Tycko, Q. Rev. Biophys. 39 (2006) 1.
[6] J.D. Sipe, A.S. Cohen, J. Struct. Biol. 130 (2000) 88.
[7] F. Immel, Y. Jiang, Y.Q. Wang, C. Marchal, L. Maillet, S. Perrett, C. Cullin, J. Biol. Chem. 282 (2007) 7912.
[8] M. Meyer-Luehmann, J. Coomaraswamy, T. Bolmont, S. Kaeser, C. Schaefer, E. Kilger, A. Neuenschwander, D. Abramowski, P. Frey, A.L. Jaton, J.M. Vigouret, P. Paganetti, D.M. Walsh, P.M. Mathews, J. Ghiso, M. Staufenbiel, L.C. Walker, M. Jucker, Science 313 (2006) 1781.
[9] R.A. Kammerer, D. Kostrewa, J. Zurdo, A. Detken, C. Garcia-Echeverria, J.D. Green, S.A. Muller, B.H. Meier, F.K. Winkler, C.M. Dobson, M.O. Steinmetz, Proc. Natl. Acad. Sci. USA 101 (2004) 4435.
[10] F. Chiti, C.M. Dobson, Annu. Rev. Biochem. 75 (2006) 333.
[11] E.D. Eanes, G.G. Glenner, J. Histochem. Cytochem. 16 (1968) 673.
[12] R. Nelson, M.R. Sawaya, M. Balbirnie, A.O. Madsen, C. Riekel, R. Grothe, D. Eisenberg, Nature 435 (2005) 773.
[13] M.R. Sawaya, S. Sambashivan, R. Nelson, M.I. Ivanova, S.A. Sievers, M.I. Apostol, M.J. Thompson, M. Balbirnie, J.J. Wiltzius, H.T. McFarlane, A.O. Madsen, C. Riekel, D. Eisenberg, Nature 447 (2007) 453.
[14] P.C.A.v.d. Wel, J.R. Lewandowski, R.G. Griffin, J. Am. Chem. Soc. 129 (2007) 5117.
[15] M. Hoshino, H. Katou, Y. Hagihara, K. Hasegawa, H. Naiki, Y. Goto, Nat. Struct. Biol. 9 (2002) 332.
[16] C. Ritter, M.L. Maddelein, A.B. Siemer, T. Luhrs, M. Ernst, B.H. Meier, S.J. Saupe, R. Riek, Nature 435 (2005) 844.
[17] A. Bockmann, C. R. Chimie 9 (2006) 381.
[18] F. Castellani, B. van Rossum, A. Diehl, M. Schubert, K. Rehbein, H. Oschkinat, Nature 420 (2002) 98.
[19] A. Lange, S. Becker, K. Seidel, K. Giller, O. Pongs, M. Baldus, Angew. Chem. Int. Ed. 44 (2005) 2089.
[20] A. Lange, K. Giller, S. Hornig, M.F. Martin-Eauclaire, O. Pongs, S. Becker, M. Baldus, Nature 440 (2006) 959.
[21] K. Seidel, M. Etzkorn, H. Heise, S. Becker, M. Baldus, Chembiochem 6 (2005) 1638.
[22] S.G. Zech, A.J. Wand, A.E. McDermott, J. Am. Chem. Soc. 127 (2005) 8618.
[23] N. Ferguson, J. Becker, H. Tidow, S. Tremmel, T.D. Sharpe, G. Krause, J. Flinders, M. Petrovich, J. Berriman, H. Oschkinat, A.R. Fersht, Proc. Nat. Acad. Sci. USA 103 (2006) 18875.
[24] H. Heise, W. Hoyer, S. Becker, O.C. Andronesi, D. Riedel, M. Baldus, Proc. Natl. Acad. Sci. USA 102 (2005) 15871.
[25] K. Iwata, T. Fujiwara, Y. Matsuki, H. Akutsu, S. Takahashi, H. Naiki, Y. Goto, Proc. Natl. Acad. Sci. USA 103 (2006) 18119.
[26] C.P. Jaroniec, C.E. MacPhee, V.S. Bajaj, M.T. McMahon, C.M. Dobson, R.G. Griffin, Proc. Natl. Acad. Sci. USA 101 (2004) 711.
[27] A.T. Petkova, R.D. Leapman, Z.H. Guo, W.M. Yau, M.P. Mattson, R. Tycko, Science 307 (2005) 262.
[28] A.T. Petkova, W.M. Yau, R. Tycko, Biochemistry 45 (2006) 498.
[29] A.B. Siemer, C. Ritter, M. Ernst, R. Riek, B.H. Meier, Angew. Chem. Int. Ed. 44 (2005) 2441.
[30] A.T. Petkova, Y. Ishii, J.J. Balbach, O.N. Antzutkin, R.D. Leapman, F. Delaglio, R. Tycko, Proc. Natl. Acad. Sci. USA 99 (2002) 16742.
[31] J.C.C. Chan, N.A. Oyler, W.M. Yau, R. Tycko, Biochemistry 44 (2005) 10669.
[32] D.D. Laws, H.M.L. Bitter, K. Liu, H.L. Ball, K. Kaneko, H. Wille, F.E. Cohen, S.B. Prusiner, A. Pines, D.E. Wemmer, Proc. Natl. Acad. Sci. USA 98 (2001) 11686.
[33] J.M. Kenney, D. Knight, M.J. Wise, F. Vollrath, Eur. J. Biochem. 269 (2002) 4159.
[34] U. Slotta, S. Hess, K. Spiess, T. Stromer, L. Serpell, T. Scheibel, Macromol. Biosci. 7 (2007) 183.
[35] I. Marcotte, J.D. van Beek, B.H. Meier, Macromolecules 40 (2007) 1995.
[36] U. Baxa, T. Cassese, A.V. Kajava, A.C. Steven, in: J.M. Squire, D.A.D. Parry, A. Kajava (Eds.), Fibrous Proteins: Amyloids, Prions and Beta Proteins, Advances in Protein Chemistry, vol. 73, Academic Press, 2006, p. 125.
[37] R. Nelson, D. Eisenberg, in: J.M. Squire, D.A.D. Parry, A. Kajava (Eds.), Fibrous Proteins: Amyloids, Prions and Beta Proteins, Advances in Protein Chemistry, vol. 73, Academic Press, 2006, p. 235.
[38] A.D. Gossert, S. Bonjour, D.A. Lysek, F. Fiorito, K. Wuthrich, Proc. Natl. Acad. Sci. USA 102 (2005) 646.
[39] D.A. Lysek, C. Schorn, L.G. Nivon, V. Esteve-Moya, B. Christen, L. Calzolai, C. von Schroetter, F. Fiorito, T. Herrmann, P. Guntert, K. Wuthrich, Proc. Natl. Acad. Sci. USA 102 (2005) 640.
[40] R. Riek, S. Hornemann, G. Wider, M. Billeter, R. Glockshuber, K. Wuthrich, Nature 382 (1996) 180.
[41] R. Zahn, A.Z. Liu, T. Luhrs, R. Riek, C. von Schroetter, F.L. Garcia, M. Billeter, L. Calzolai, G. Wider, K. Wuthrich, Proc. Natl. Acad. Sci. USA 97 (2000) 145.
[42] L. Bousset, F. Briki, J. Doucet, R. Melki, J. Struct. Biol. 141 (2003) 132.
[43] L. Bousset, N.H. Thomson, S.E. Radford, R. Melki, Embo J. 21 (2002) 2903.
[44] N. Fay, V. Redeker, J. Savistchenko, S. Dubois, L. Bousset, R. Melki, J. Biol. Chem. 280 (2005) 37149.
[45] A.V. Kajava, U. Baxa, R.B. Wickner, A.C. Steven, Proc. Natl. Acad. Sci. USA 101 (2004) 7885.
[46] A.V. Kajava, A.C. Steven, in: J.M. Squire, D.A.D. Parry, A. Kajava (Eds.), Fibrous Proteins: Amyloids, Prions and Beta Proteins, Advances in Protein Chemistry, vol. 73, Academic Press, 2006, p. 55.
[47] A. Balguerie, S. Dos Reis, C. Ritter, S. Chaignepain, B. Coulary-Salin, V. Forge, K. Bathany, I. Lascu, J.M. Schmitter, R. Riek, S.J. Saupe, Embo J. 22 (2003) 2071.
[48] S.J. Saupe, Microbiol. Mol. Biol. Rev. 64 (2000) 489.
[49] S. Dos Reis, B. Coulary-Salin, V. Forge, I. Lascu, J. Begueret, S.J. Saupe, J. Biol. Chem. 277 (2002) 5703.
[50] M.L. Maddelein, S. Dos Reis, S. Duvezin-Caubet, B. Coulary-Salin, S.J. Saupe, Proc. Natl. Acad. Sci. USA 99 (2002) 7402.

[51] A. Sen, U. Baxa, M.N. Simon, J.S. Wall, R. Sabate, S.J. Saupe, A.C. Steven, J. Biol. Chem. 282 (2007) 5545.
[52] A.B. Siemer, A.A. Arnold, C. Ritter, T. Westfeld, M. Ernst, R. Riek, B.H. Meier, J. Am. Chem. Soc. 128 (2006) 13224.
[53] A. Lange, S. Luca, M. Baldus, J. Am. Chem. Soc. 124 (2002) 9704.
[54] A. Lange, K. Seidel, L. Verdier, S. Luca, M. Baldus, J. Am. Chem. Soc. 125 (2003) 12640.
[55] M. Etzkorn, A. Bockmann, A. Lange, M. Baldus, J. Am. Chem. Soc. 126 (2004) 14746.
[56] O.C. Andronesi, S. Becker, K. Seidel, H. Heise, H.S. Young, M. Baldus, J. Am. Chem. Soc. 127 (2005) 12965.
[57] J. Heller, A.C. Kolbert, R. Larsen, M. Ernst, T. Bekker, M. Baldwin, S.B. Prusiner, A. Pines, D.E. Wemmer, Protein Sci. 5 (1996) 1655.